Hypersound anomalies and elastic constants in single-crystal PbMg1/3Nb2/3O3 by Brillouin scattering

C.-S. Tu, V. Hugo Schmidt, and I. G. Siny

Citation: Journal of Applied Physics **78**, 5665 (1995); doi: 10.1063/1.359622
View online: http://dx.doi.org/10.1063/1.359622
View Table of Contents: http://scitation.aip.org/content/aip/journal/jap/78/9?ver=pdfcov
Published by the AIP Publishing

Hypersound anomalies and elastic constants in single-crystal $PbMg_{1/3}Nb_{2/3}O_3$ by Brillouin scattering

C.-S. Tu,[a] V. Hugo Schmidt, and I. G. Siny[b]
Department of Physics, Montana State University, Bozeman, Montana 59717

(Received 28 December 1994; accepted for publication 5 July 1995)

The longitudinal (LA) and transverse (TA) Brillouin spectra along [001] phonon direction have been measured as a function of temperature (50–475 K) in single-crystal $PbMg_{1/3}Nb_{2/3}O_3$ with scattering angles $\theta_s=180°$ and $32.5\pm0.2°$. The Brillouin frequency shift with decreasing temperature shows a broad softening anomaly for both LA and TA phonon modes. For $\theta_s=180°$, a gradual growth in damping with maximum near 270 K is observed and is attributed to order parameter fluctuations. An additional Landau–Khalatnikov maximum is also observed at $T_c\sim212$ K. This anomaly implies a rapid growth of ferroelectric ordering near T_c and is consistent with the earlier linear birefringence results reported by Westphal *et al.* The elastic stiffness and compliance constants, C_{11}^E, C_{44}^E, and s_{44}^E are also determined between 200 and 370 K. © *1995 American Institute of Physics.*

I. INTRODUCTION

Relaxor ferroelectrics generally mean the complex perovskites with ABO_3-type unit cell and are crystals in which unlike-valence cations belonging to a given site (A or B) are presented in the correct ratio for charge balance, but are situated randomly on these cation sites. These randomly different cation charges give rise to random fields. These random fields tend to make the phase transitions "diffuse" instead of sharp as in normal ferroelectrics.[1] The physical properties of relaxor ferroelectrics near transitions also depend on the cation ordering degree. The ordering tendency depends on several things such as method of crystal growth, cation valence, and thermal treatment (e.g., quenching or annealing). Another complication is the aging effect which can span a wide time scale in a nonlinear manner.[1]

In the supposedly disordered $PbMg_{1/3}Nb_{2/3}O_3$ (PMN) crystal, and unexpected microstructure on a nanometric length scale with 1:1 B':B'' cation ordering was reported.[2] Such 1:1 ordering, when charge neutrality requires 1:2 stoichiometry, implies locally charged regions causing fields which can induce order parameter fluctuations. Recent measurements indicate only a 5% tendency toward 1:1 ordering in these microregions.[3] Three recent models for relaxor PMN have been proposed, namely the random field (RF) model of Westphal *et al.*,[4] the dipolar glass model of Viehland *et al.*,[5] and the structural model by Mathan *et al.*[6] This last model indicates an average cubic structure even at 5 K, but with some 20% of the material in noncubic FE microdomains near 100 Å size.

The RF model postulates random electric fields originating in a peculiarity of PMN's structure (local nonstoichiometric order causing local net charge), resulting in microdomains polarized along eight ⟨111⟩ directions. The authors also postulate that the cubic anisotropy corresponding to these eight directions is low enough so that the random fields can suppress the FE transition.[4] In the dipolar glass model, the "pseudospins" are nanometer-sized superparaelectric clusters which correspond to the microdomains in the RF model. The dipolar glass model assumes these clusters can flip at higher temperature, but freeze into a random configuration at lower temperature.

II. EXPERIMENT

In this study, a single-crystal of $PbMg_{1/3}Nb_{2/3}O_3$ with size of $5.37\times4.77\times2.82$ $(mm)^3$ was used for Brillouin scattering with scattering angles $\theta_s=180°$ and $32.5\pm0.2°$. Here θ_s is the angle between incident and scattered wave vectors inside the crystal. In order to reduce the low-lying frequency mode of the Raman spectra, a narrow-band (1 Å) interference filter was used. The sample which was used for previous Raman scattering[7] was oriented so as to allow observation of [001] phonons for both scattering angles. The light source was a Lexel Model 95-2 argon laser with $\lambda=514.5$ nm at a power of ~100 mW. Scattered light was analyzed by a Burleigh five-pass Fabry–Perot interferometer. A Leybold RGD-210 closed-cycle helium refrigerator was used with a LakeShore DRC-91C temperature controller. The temperature was measured within ±0.01 K by a calibrated silicon diode thermal sensor. The sample was heated from 50 to 475 K by steps and results were found to be reproducible.

For determination of natural-phonon half width, the natural-phonon spectrum, and the instrumental function were assumed to have the Lorentz distribution, and the broadening due to collection optics was assumed to have rectangular distribution. In this case, the natural-phonon half-width $\delta\nu_{ph}$ is given by[8]

$$\delta\nu_{ph}=(\delta\nu_{obs}^2-\delta\nu_{ang}^2)^{1/2}-\delta\nu_{inst}, \tag{1}$$

where $\delta\nu_{obs}$, $\delta\nu_{inst}$, and $\delta\nu_{ang}$ represent the observed, instrumental, and collection optics half widths, respectively. The half width of the Rayleigh line from fused quartz (which had approximately the assumed Lorentz shape) was taken as the instrumental broadening $\delta\nu_{inst}\sim0.02$ FSR. Here FSR means the free spectral range, 17.035 GHz. The Brillouin line

[a]Present address: Dept. of Physics, Fu-Jen University, Taipei, Taiwan.
[b]Now returned to A. F. Ioffe Physical Tech. Inst. RAS, St. Petersburg, Russia.

 0021-8979/95/78(9)/5665/4/$6.00

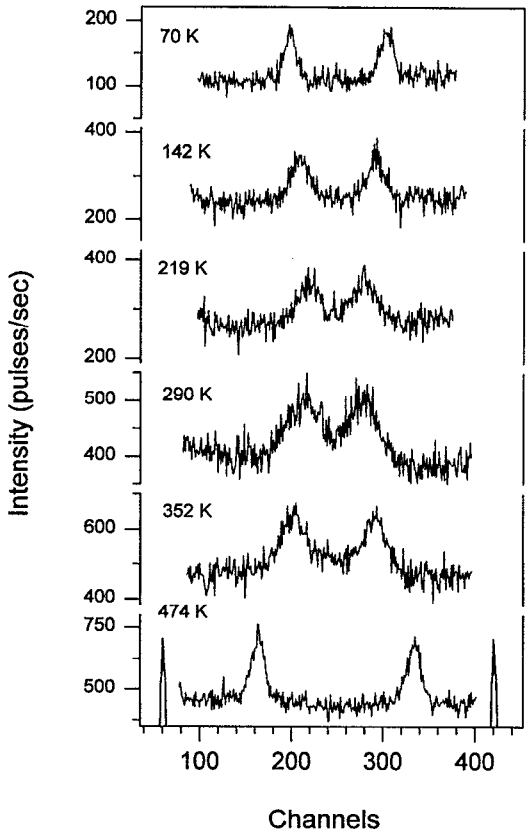

FIG. 1. Anti-Stokes and Stokes components of the LA[001] Brillouin spectra for temperatures near the maximum damping for $\theta_s=180°$. The frequency interval between the two Rayleigh peaks is 17.035 GHz (FSR).

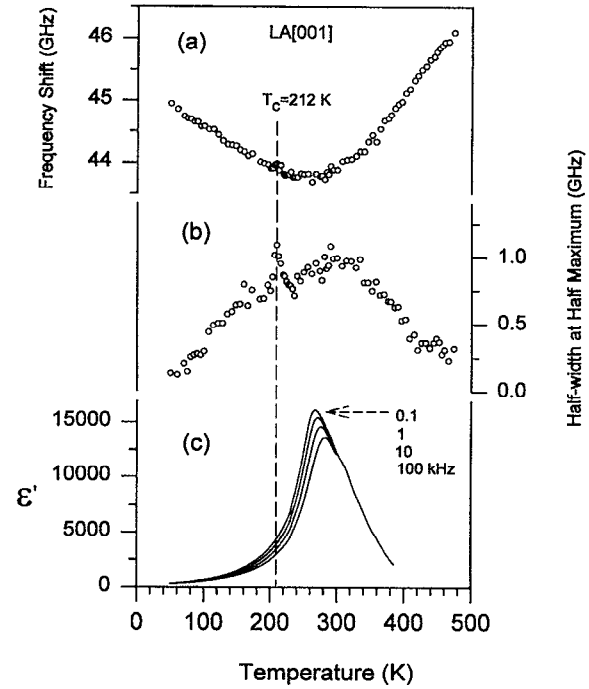

FIG. 2. (a) Frequency shift $\Delta\nu$ and (b) half-width $\delta\nu_{ph}$ vs temperature of the LA[001] phonons for $\theta_s=180°$. (c) The real part of dielectric permittivity vs temperature at four different frequencies. The dashed line indicates the ferroelectric phase transition temperature $T_c\sim212$ K.

broadening $\delta\nu_{ang}$ due to finite collection angle $\delta\theta_{ap}$ is described by a well-known formula[9] which to second order in $\delta\theta_{ap}$ is

$$\frac{\delta\nu_{ang}}{\Delta\nu}=\frac{\cot(\theta/2)\,\delta\theta_{ap}}{2}-\frac{(\delta\theta_{ap})^2}{8}, \tag{2}$$

where θ is the scattering angle and $\Delta\nu$ is the Brillouin frequency shift.

III. RESULTS AND DISCUSSION

Actual LA[001] phonon spectra of the anti-Stokes and Stokes Brillouin components for $\theta_s=180°$ are shown in Fig. 1. According to the calculations of Ref. 10, there is no transverse mode to be expected in this configuration. The data shown here are for several temperatures near the maximum value of half width. Both frequency shift and half width exhibit a strong temperature dependence. Figure 1 also shows that the background of the Brillouin spectra changes drastically with temperature. Since Brillouin spectra are sensitive to the central peak near the brillouin zone center, this background anomaly implies an evolution of the central component.

The accumulated data for backscattering ($\theta_s=180°$) are shown in Fig. 2. Here, the Lorentz profile was used to fit the phonon spectra, from which the frequency shift and half width were obtained. Figure 2 data indicate that a broad phonon softening occurs starting at $T>475$ K and reaches a minimum near 270 K, associated with a broad maximum in damping. The temperature dependences of velocity and damping look like reflections of each other. Such a growth of damping over a wide temperature range reveals that order parameter fluctuations are the dominant dynamic mechanism. The dynamic fluctuation contribution is a characteristic of an $\eta^2\mu$-type quadratic coupling (electrostriction),[11] squared in order parameter and linear in strain. However, a step-like frequency softening typical for $\eta^2\mu$-type coupling is not observed in this case.[11] Beside this broad damping background, there is an additional sharp damping peak near 212 K which can be connected with the typical Landau–Khalatnikov maximum. For comparison, frequency-dependent dielectric measurements were also carried out by ourselves and are presented in Fig. 2(c).

What are the origins of these two damping peaks in PMN? The temperature dependence of the linear birefringence Δn in PMN under an external electric field suggests an equilibrium phase transition temperature T_c in the absence of a random field, 200 K$<T_c<$234 K.[4] In addition, by fitting the time dependence of the linear birefringence with two different exponents β below and above 212 K, Westphal *et al.* propose that the Curie temperature of PMN is $T_c\sim212$ K.[4] Viehland *et al.* also claim that the freezing temperature is $T_f\sim217$ K below which a dramatic change of the relaxation time distribution is observed which is interpreted as a result of a long-range correlation of polar microdomains.[5] Recent quasielastic-neutron scattering[12] on PMN supports the above

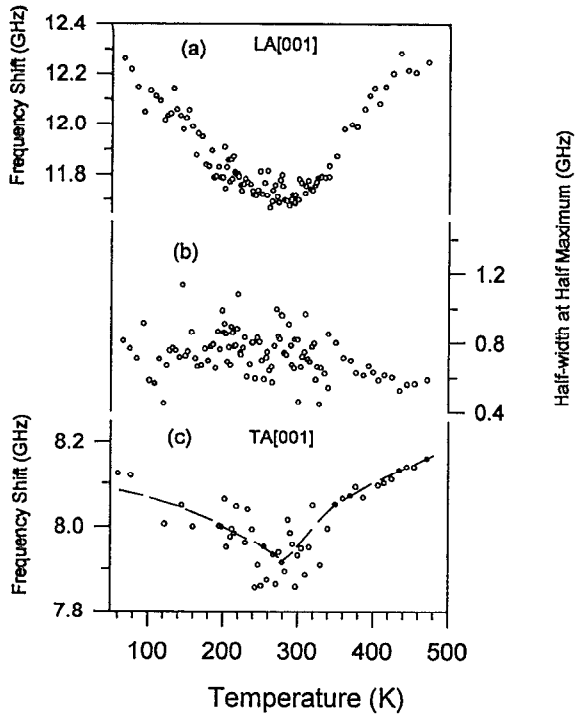

FIG. 3. (a) Frequency shift $\Delta\nu$ and (b) half-width $\delta\nu_{\text{obs}}$ vs temperature of the LA[001] phonons for $\theta_s=32.5\pm0.2°$. (c) Frequency shift vs temperature of the TA[001] phonons. The dashed line is a guide to the eye.

interpretations and shows that the correlation length is nearly temperature independent with a maximum value of 200 Å below ~217 K. Since the Landau–Khalatnikov maximum is sensitive to the occurrence of FE ordering,[8] we attribute this Landau–Khalatnikov maximum in PMN to the rapid growth of FE ordering at $T_c\sim212$ K.

The random field model[4] proposes that the dielectric diffuse phase transition near 270 K is due to quenched random electric fields originating from charged compositional fluctuations at the B site of the ABO_3 structure.[4] These random fields can suppress a long-range-order ferroelectric transition and generate order parameter fluctuations. Thus, one can expect that such random fields are responsible for the evolution of broad damping background with a maximum near 270 K [see Fig. 2(b)] and the modification of $\eta^2\mu$-type frequency softening, i.e., a broad dip instead of a typical step-like anomaly. Similar acoustic anomalies, i.e., a broad damping maximum and a broad velocity dip, are also observed in $Na_{1/2}Bi_{1/2}TiO_3$ (NBT).[13,14] However, the usual Landau theory does not predict these anomalies.[15] Such acoustic similarity between PMN and NBT seems to imply the importance of randomly placed cations in complex relaxor ferroelectrics.

The longitudinal LA[001] and transverse TA[001] phonon data for angle $\theta_s=32.5\pm0.2°$ are shown in Fig. 3. A phonon frequency softening is also observed for both LA and TA phonon modes, with a broad minimum at $T\sim270$ K. According to Eq. (2), the relative error in damping for the small-angle scattering is much larger than for backscattering, and is comparable to both $\delta\nu_{\text{ph}}$ and $\delta\nu_{\text{inst}}$, so the natural-phonon half-width $\delta\nu_{\text{ph}}$ for this small angle cannot be determined accurately.

IV. CALCULATIONS OF ELASTIC CONSTANTS

Brillouin light scattering is a powerful tool to determine the elastic stiffness and compliance constants. In general, the equation of motion for a phonon propagating in a piezoelectric material can be written as a 3×3 eigenvalue equation[16]

$$\rho V_q^2 u_i=\Gamma_{ijkl}q_jq_lu_k,\quad \Gamma_{ijkl}=C^E_{ijkl}+\frac{e_{\alpha ij}e_{jkl}}{\epsilon^s_{j\alpha}},\tag{3}$$

where V_q and u_i are the phonon velocity and displacement (polarization), respectively; Γ_{ijkl} is the piezoelectrically stiffened elastic modulus;[16] ρ is the sample density; C^E_{ijkl} is the elastic stiffness constant at constant electric field; $e_{\alpha ij}$ is the piezoelectric stress constant; $\epsilon^s_{j\alpha}$ is the permittivity at constant strain; and q_j (or q_l) is the projection of the unit phonon wave vector along the ith axis.

The high-temperature phase in PMN is cubic with point group m3m whereas below 200 K, a small portion exhibited trigonal distortion as observed by Shebanov *et al.*[17] Thus, we can consider PMN as cubic for $T\geqslant200$ K. In other words, for $T\geqslant200$ K, all elements of e_{rij} are zero[18] and the nonvanishing C^E_{ijkl}, in Voigt notation, are C^E_{11}, C^E_{12}, and C^E_{44}, i.e.,[18]

$$C^E_{ij}=\begin{bmatrix} C^E_{11} & C^E_{12} & C^E_{12} & 0 & 0 & 0\\ C^E_{12} & C^E_{11} & C^E_{12} & 0 & 0 & 0\\ C^E_{12} & C^E_{12} & C^E_{11} & 0 & 0 & 0\\ 0 & 0 & 0 & C^E_{44} & 0 & 0\\ 0 & 0 & 0 & 0 & C^E_{44} & 0\\ 0 & 0 & 0 & 0 & 0 & C^E_{44}\end{bmatrix}.$$

Here, the relations $C^E_{33}=C^E_{22}=C^E_{11}$ and $C^E_{66}=C^E_{55}=C^E_{44}$ have been used for the cubic case.[18] For an arbitrary phonon wave direction $\bar{q}$ in the crystal with cubic symmetry. Equation (3) gives a secular equation

$$\begin{vmatrix} C_{11}q_1q_1+C_{44}q_3q_3+C_{44}q_2q_2-\rho V^2 & C_{12}q_1q_2+C_{44}q_2q_1 & C_{12}q_1q_3+C_{44}q_3q_1\\ C_{44}q_1q_2+C_{12}q_2q_1 & C_{44}q_1q_1+C_{11}q_2q_2+C_{44}q_3q_3-\rho V^2 & C_{12}q_2q_3+C_{44}q_3q_2\\ C_{44}q_1q_3+C_{12}q_3q_1 & C_{44}q_2q_3+C_{12}q_3q_2 & C_{44}q_2q_2+C_{11}q_3q_3+C_{44}q_1q_1-\rho V^2\end{vmatrix}=0.\tag{4}$$

TABLE I. Elastic stiffness and compliance constants of PMN at several temperatures from two scattering angles $\theta_s=180°$ and $32.5\pm0.2°$.

	From $\theta_s=180°$	From $\theta_s=32.5\pm0.2°$		
T(K)	$C_{11}^E(10^{11}$ N/m$^2)$	$C_{11}^E(10^{11}$ N/m$^2)$	$C_{44}^E(10^{10}$ N/m$^2)$	$s_{44}^E(10^{-11}$ m^2/N)
200	1.64	1.52	6.93	1.44
219	1.63	1.49	6.96	1.44
245	1.63	1.48	6.68	1.50
268	1.62	1.49	6.76	1.48
284	1.62	1.47	6.69	1.50
300	1.62	1.49	6.76	1.48
321	1.63	1.49	6.96	1.44
340	1.64	1.49	6.87	1.46
370	1.67	1.55	7.00	1.43

This secular equation yields three eigenvalues which are associated with sound velocities of three phonon waves propagating in the same direction, and three mutually orthogonal eigenvectors which are the polarizations (displacement) of phonon. In our experimental situation, the measured phonon is along the [001] direction ($\tilde{q}\|[001]$),[7] i.e., $q_3=1$, $q_1=q_2=0$. By solving the secular Eq. (4), one can obtain

$$\rho V_{\mathrm{LA}}^2=C_{11}^E;\quad \rho V_{\mathrm{TA}}^2=C_{44}^E. \tag{5}$$

Subscripts LA and TA represent the longitudinal and transverse acoustic phonon modes, respectively. Since the thermal strain $\Delta L/L_0$ is almost zero below 400 K,[1] one can use the density of PMN at room temperature, i.e., $\rho=8.12\times10^3$ kg/m^3,[19] for calculation of elastic constants below 400 K. The relation between frequency shift and sound velocity is[20]

$$V=\frac{\lambda_0\Delta\nu}{2n\,\sin(\theta/2)}, \tag{6}$$

where λ_0 is the wavelength of the incident light in vacuum, and θ is the scattering angle in the crystal. Substituting Eq. (6) into Eq. (5), we have

$$C_{11}^E=\rho\left(\frac{\lambda_0\Delta\nu_{\mathrm{LA}}}{2n\,\sin(\theta/2)}\right)^2;\quad C_{44}^E=\rho\left(\frac{\lambda_0\Delta\nu_{\mathrm{TA}}}{2n\,\sin(\theta/2)}\right)^2; \tag{7}$$

where $\Delta\nu_{\mathrm{LA}}$ and $\Delta\nu_{\mathrm{TA}}$ are the longitudinal and transverse phonon frequency shifts, respectively. The temperature dependent refractive index $n(T)$ is obtained from Ref. 21. The calculated values of C_{11}^E, C_{44}^E, and s_{44}^E at several temperatures are listed in Table I. The error in these elastic constants is about 1.3%. Here the relation $s_{44}^E=1/C_{44}^E$, has been used to obtain s_{44}^E.[16]

As seen in Table I both elastic stiffness constants C_{11}^E and C_{44}^E show a slight softening around 280 K. The values of C_{11}^E from $\theta_s=180°$ and $\theta_s=32.5\pm0.2°$ are in good agreement with each other. Since sound velocity is sensitive to scattering angle, we attribute the slight difference in C_{11}^E to the determination error for small scattering angle.

At room temperature, the elastic stiffness constant C_{11}^E of PMN is smaller compared to those of pure perovskite-type ferroelectrics. For instance, C_{11}^E is 2.35×10^{11} N/m^2 for $PbTiO_3$ and 2.11×10^{11} N/m^2 for $BaTiO_3$.[20] However, the elastic stiffness constant C_{44}^E of PMN is slightly greater than those of $PbTiO_3$ ($C_{44}^E=6.51\times10^{10}$ N/m^2) and $BaTiO_3$ ($C_{44}^E=5.62\times10^{10}$ N/m^2).[20]

V. CONCLUSIONS

A broad phonon softening has been observed for both LA[001] and TA[001] phonon modes starting at $T>475$ K followed by a hardening around 270 K. For scattering angle $\theta_s=180°$, a strong broad damping background is observed and is attributed to order parameter fluctuations. Such fluctuations are attributed to random fields originating from random placed cations at the B site of the ABO_3 structure. An additional Landau–Khalatnikov maximum is also observed at $T_c\sim212$ K and implies a rapid growth of FE ordering. In brief, the present Brillouin scattering results favor the random field model.[4] The similarity between PMN and NBT implies that the random-cations-caused fluctuations play an important role in the acoustic anomalies of complex relaxor ferroelectrics.

ACKNOWLEDGMENTS

This work was supported in part by NSF Grant No. DMR-9017429 and DOE Equipment Grant No. FG05-91ER79046.

[1] L. E. Cross, Ferroelectrics **76**, 241 (1987).
[2] A. D. Hilton, D. J. Barber, C. A. Randall, and T. R. Shrout, J. Mater. Sci. **25**, 3461 (1990).
[3] S. B. Vakhrushev, A. A. Nabereznov, Y. P. Feng, S. K. Sinha, S. M. Shapiro, T. Egami, H. D. Rosenfeld, and D. E. Moncton, Bull. Am. Phys. Soc. **39**, 680 (1994).
[4] V. Westphal, W. Kleemann, and M. D. Glinchuk, Phys. Rev. Lett. **68**, 847 (1992).
[5] D. Viehland, M. Wuttig, and L. E. Cross, Ferroelectrics **120**, 71 (1991).
[6] N. de Mathan, E. Husson, G. Calvarin, J. R. Gavarri, A. W. Hewat, and A. Morell, J. Phys. Condens. Matter **3**, 8159 (1991).
[7] I. G. Siny and T. A. Smirnova, Ferroelectrics **90**, 191 (1989).
[8] T. Hikita, J. Phys. Soc. Jpn. **53**, 1513 (1984).
[9] J. M. Vaughan, *The Fabry-Perot Interferometer* (Adam Hilger, Bristol and Philadelphia, 1989), pp. 341–344; H. G. Danielmeyer, J. Acoust. Soc. Am. **47**, 151 (1970).
[10] R. Vacher and L. Boyer, Phys. Rev. B **6**, 639 (1972).
[11] W. Rehwald, Adv. Phys. **22**, 721 (1973).
[12] S. Vakhrushev, B. Kryatkovsky, A. Naberzhou, N. Okuneva, and B. Topervers, Ferroelectrics **90**, 173 (1989).
[13] C.-S. Tu, I. G. Siny, and V. H. Schmidt, Ferroelectrics **152**, 403 (1994).
[14] C.-S. Tu, I. G. Siny, and V. H. Schmidt, Phys. Rev. B **49**, 11550 (1994).
[15] W. Yao, H. Z. Cummins, and R. H. Bruce, Phys. Rev. B **24**, 424 (1981); J. J. L. Horikx, A. F. M. Arts, J. I. Dijkhuis, and H. W. de Wijn, *ibid.* **39**, 5726 (1989).
[16] E. Dieulesaint and D. Royer, *Elastic Waves in Solids* (Wiley, New York, 1982), pp. 244–269.
[17] L. A. Shebanov, P. Kaspostins, and J. Zvirgzds, Ferroelectrics **56**, 1057 (1984).
[18] J. F. Nye, *Physical Properties of Crystals* (Clarendon, Oxford, 1957).
[19] Landolt-Bornstein, *New Series*, Vol. III/16a, edited by K.-H. Hellwege (Springer, Berlin, 1982).
[20] Z. Li, M. Grimsditch, X. Xu, and S.-K. Chan, Ferroelectrics **141**, 313 (1993).
[21] G. Burns and F. H. Dacol, Solid State Commun. **48**, 853 (1983).